Introduction

Ray-based reflection tomography has become widely used as a tool for updating velocity models in depth imaging. Historically, development of ray-based tomography for depth imaging followed two separate methodologies. Early ray-based tomography was based on differences in traveltime observed between modeled data and actual seismic data (Bishop et al, 1983). As technology for imaging in complex areas progressed, however, it became more difficult to obtain reliable time differences on input data, and hence an alternative methodology based on residual moveout on migrated offset gathers was developed (Stork, 1992).

Today, the success of wavefield-extrapolation methods in imaging has created a corresponding interest in extending these methods to accomplish velocity updating as well. The primary motivation is to remove the underlying dependence of tomography on raytracing. Just as in the ray-based case, two methodologies for wavefield-extrapolation tomography are emerging. The first is based on wavefield differences between forward modeled data and seismic data (Tarantola, 1984), referred to as waveform tomography, while the second and more recent methodology is based on a residual obtained from migrated gathers, and is referred to as wave-equation velocity analysis (Biondi and Sava, 1999, Sava and Biondi, 2004), or one-way waveform inversion (Shen et al, 2003).

In this paper our primary focus is on wave-equation velocity analysis: obtaining velocity updates from information on migrated gathers. In what follows, we give a general description of the methodology, as well as 3D data and 2D synthetic examples to illustrate various aspects of the technique.

Velocity backprojection from image differencing

Wave-equation velocity analysis is based on the general principle that a change to a velocity model will result in a change in the image. Suppose we are given a downward-continued migrated image $I_c(x,z,h)$ that is a function of space and downward-continued offset (which we refer to as image-offset to distinguish it from offset at the surface). Suppose also that this image is obtained using the correct velocity model. If a slowness change δc is made to the correct model to produce a new image I, then in the linear approximation the difference in images is related to the slowness perturbation by

$$I - I_c \equiv \delta I = \frac{\partial I}{\partial c}\delta c \equiv S\delta c\,, \qquad (1)$$

where for simplicity we shall refer to S as the scattering operator. The goal of wave-equation velocity analysis is to solve this equation for δc given a suitable image difference δI. Since the inverse to the scattering operator cannot be found in general, the solution of eqn. (1) is done iteratively in the least-squares sense. The image difference is treated as a residual, and an initial estimate δc^* of δc is computed by taking the adjoint of the scattering operator and applying it to the image residual, so that $\delta c^* = S^* \delta I$. This is then used to compute a new slowness update and residual using either a linear or nonlinear solver, such as a conjugate-gradient solver. As the procedure iterates, the residual decreases to a minimum that is ideally zero. Since the procedure is least squares, it also minimizes an objective function $J(c) = |\delta I|^2$, which is short-hand for squaring each sample in the image difference and summing over all space and offset. If one varies the objective function with respect to the slowness, one essentially obtains $\delta c^* = S^* \delta I$ back again. For this reason, the initial estimate of the slowness perturbation δc^* is often referred to as the gradient of the objective function. Overall, this technique is a member of a class of inversion methods generally referred to as adjoint methods, since the adjoint of the scattering operator is used in its construction.

Backprojection of image differences using downward and upward continuation can be effective in recovering slowness perturbations, and is particularly applicable to areas where such image differences are directly available, such as a 4D workflow. An actual data test example in 3D of the use of an image difference to recover a slowness perturbation is illustrated in Figure 1.

Velocity backprojection from focusing: using the migrated gathers

In most cases outside of 4D, a direct image difference will not be available for backprojection. For these cases a different residual wavefield based on a different objective function must be selected (Peng et al, 2003). Consider the downward-extrapolated wavefield $\psi(x,h,z,t)$ as a function of space, image-offset, and time. The driving principle for the derivation of a suitable residual wavefield can be found in Claerbout's survey-sinking principle, which states that downward-continued sources and receivers spatially coincide at zero time if the velocity model is correct. According to Claerbout's principle, the correct velocity model is one for which all energy is optimally focused at zero offset and zero time. If the model is incorrect, the energy will not focus. It is therefore reasonable to assume that *the wavefield remaining when all focused energy is removed from an image is a direct measure of model fitness*. Such wavefields can be used as residual wavefields for velocity backprojection, in an analogous procedure to that outlined in the previous section. Mathematically, the principle can be stated by assuming there exists an operator H that annihilates the correct image (i.e. removes all focused energy), but leaves unfocused energy untouched. This means that $HI_c = 0$, but $HI \neq 0$. If we multiply eqn. (1) by H we obtain $HI = HS\delta c$. What is of primary importance here is that this equation no longer explicitly involves the correct image. Hence we can solve for the slowness perturbation directly in the adjoint sense to give

$$\delta c^* = (HS)^* HI \,. \qquad (2)$$

This equation gives a general principle for velocity backprojection in order to optimize focusing in the image.

How does the notion of optimal focusing correspond to the standard notion of flattening of migrated image gathers? The correspondence is direct in the case of angle gathers because the image-offset and angle domains are related by slant stacking. We illustrate this in the example in Figure 2 below, where a simple elliptical slowness anomaly is backprojected using eqn. (2). The modeled data in this case was created with the anomaly present, and the initial migration was done with a constant-velocity background. Examination of the gathers prior to the update reveals substantial energy that has not focused in the image-offset domain. This shows up as elliptical 'tails' extending from the focused energy away from zero offset. In the angle domain after slant stack, these 'tails' show up as complex residual moveout, which can be seen in the corresponding angle gather. After removal of the focused energy, which leaves just the tails, the remaining wavefield can be used as a residual field in an iterative backprojection process using eqn. (2). Migration with the final model shows that the tails have now disappeared, the energy is well focused, and after slant stack, the image gathers are flat. This illustrates the elegant correspondence between optimal focusing in the offset domain, and the flattening of gathers, which is a necessary condition for model correctness.

In practice there are many choices for the operator H that annihilate the correct image to varying degrees. Biondi and Sava (1999) use velocity perturbations of the background model which produce linearized image perturbations. A laterally varying residual field is then constructed by locally merging image perturbations for which gathers are locally flattest, leading to improved focusing in the update. In contrast, Shen et al (2003) use differential semblance, where H amounts to multiplication by offset in the image-offset domain. Since

multiplication by offset annihilates the wavefield at zero offset, differential semblance effectively removes focused energy from the migrated image directly. In the angle domain, this is equivalent to subtracting a given trace in the angle gather from its nearest neighbor. It is clear that the residual field obtained in this way is minimal when the gather is flat, assuming that the waveform along the gather is not significantly distorted due to illumination or AVA effects. Here we have used a similar residual field to obtain the result in Figure 2. Another example of our technique is shown in Figure 3, where the perturbation from Figure 1 was used to generate synthetic data. This data was migrated with the background velocity, the focused energy was removed to create the residual, which was then backprojected. This result gives a comparison of resolution obtained from the gathers in 2D as opposed to a direct image difference in 3D, seen in Figure 1. In both cases in Figures 2 and 3, the gathers after backprojection were essentially flat.

It is worth noting that wave-equation velocity analysis via optimal focusing differs significantly from ray-based tomography in that in principle no picking of gathers is required. Hence backprojection may be possible where structure is complex enough to make picking quite difficult. However, in practice this raises the issue of what the proper preconditioning of gathers for the residual field should be, since significant preconditioning of gather picks is often necessary for ray-based tomography. This remains an open question for further research.

In summary, we have outlined general methodologies for wave-equation velocity analysis based on both image differencing and optimal focusing using one-way wavefield extrapolation. Results on 3D data and 2D synthetics indicate that the methods are effective for the recovery of complex velocity anomalies in relatively simple background media. The suitability of these methods for more complex areas is currently under investigation.

Acknowledgements

The authors wish to thank BP's Exploration Production Technology Group for their support and permission to publish this work. We would also like to thank Laurent Sirgue, Sverre Brandsberg-Dahl, Ken Matson, and Ray Abma for useful conversations related to this work. Special thanks to Frederic Billette for his guidance, and to Bill Symes for several helpful discussions.

References

Bishop, T., Bube, K., Cutler, R., Langan, R., Love, P., Resnick, J., Shuey, R., Spindler, D., and Wyld, H., (1985): *Tomographic determination of velocity and depth in a laterally varying media*, Geopysics **50**, p. 903-923

Biondi, B. and Sava, P. (1999): *Wave-equation migration velocity analysis*, 69th Ann. Internat. Mtg., Soc. Expl. Geophys., Expanded Abstracts.

Sava, P., and Biondi, B., (2004): *Wave-equation migration velocity analysis. I. Theory*, Geophysical Prospecting **52**, 593-606

Shen, P., Stolk, C., and Symes, W., (2003): *Automatic velocity analysis by differential semblance optimization*, 73rd Ann. Internat. Mtg., Soc. Expl. Geophys., Expanded Abstracts.

Stork, C., (1988): *Reflection tomography in the post-migrated domain*, Geophysics **57**, p. 680-692

Tarantola, A., (1984): *Inversion of seismic reflection data in the acoustic approximation*, Geophysics **49**, p. 1259-1266

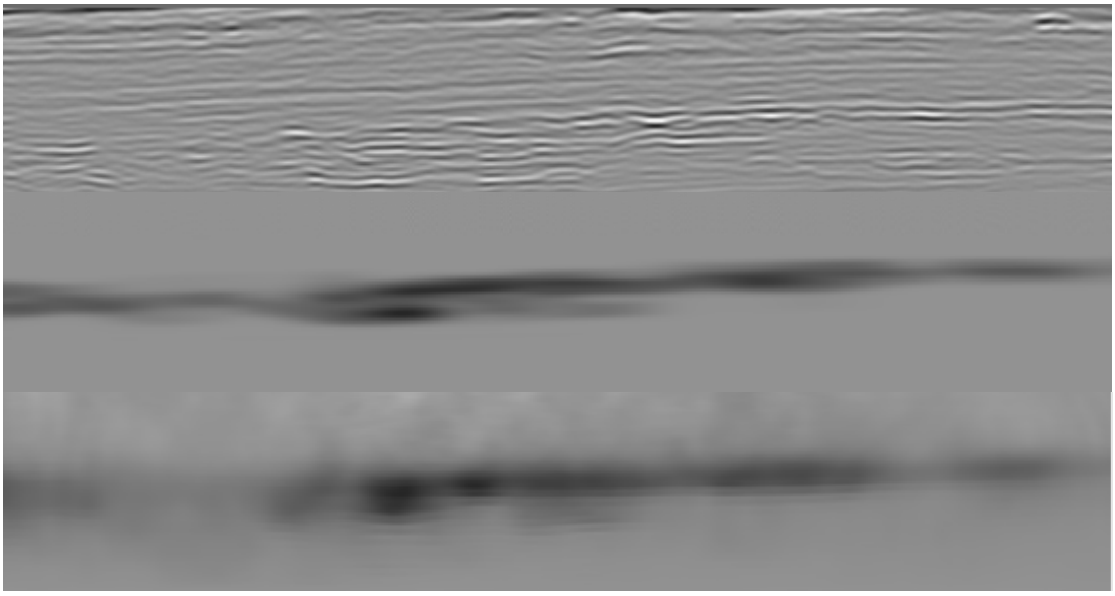

Figure 1: 3D prestack wave-equation velocity backprojection from an image difference. Figure 1a (top) shows a section with significant anhydrite layering. Figure 1b (middle) is an interpretation of the slowness perturbation associated with the anhydrites, which represents about a 10 percent variation from the background. Migrations of seismic data with and without the perturbation were done, and the image difference was obtained and backprojected using a common-azimuth wavefield-extrapolation algorithm. The result is seen in Figure 1c (bottom). The vertical extent of this window is about 1200m at a depth of about 3000m, with maximum offset 3000m.

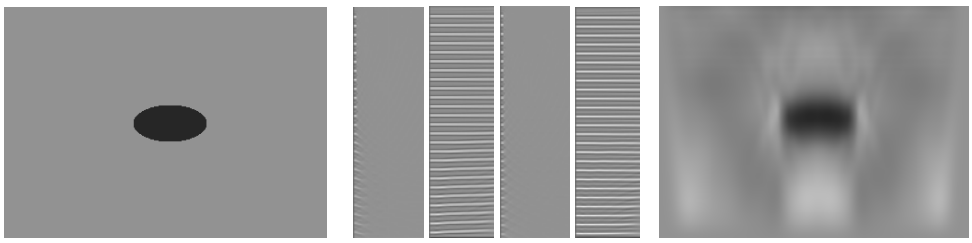

Figure 2: Sharp velocity anomaly backprojection. Figure 2a (left) shows a 10 percent elliptical slowness anomaly. The model extent is 800m horizontal by 250m vertical, with a backgoround velocity of 2000m/s. Figure 2b (four gathers) shows a comparison of gathers near the left edge of the anomaly before and after the update. Gather 1 (left) is the image-offset gather, exhibiting tails due to improper focusing. Gather 2 is the corresponding angle gather with complex moveout. Gather 3 is the image-offset gather after the update, indicating the energy is now well focused. Gather 4 is the corresponding angle gather, which is now flat. Figure 2c (right) shows the recovered slowness. Double-downward continuation was used for this example

Figure 3: 2D prestack wave-equation velocity backprojection from image gathers. Synthetic data was generated using a velocity model that contained the slowness perturbation in Figure 1b and flat reflectors. The data were then migrated using the background model, and a residual field from gathers was created by eliminating focused energy from the image-offset gathers. The result shown is the result of the backprojection of this residual, which can be compared with figures 1b and 1c above. Migrated angle gathers near the center the section before and after the update are shown on the right.